22.1

Optimization and Design of Conductivity Profiles for the PML Boundary Condition and Its Application to Bioelectromagnetic Problems

Gianluca Lazzi, Cynthia M. Furse, and Om P. Gandhi
Department of Electrical Engineering
University of Utah
Salt Lake City, UT 84112

Introduction

Berenger's Perfect Matched Layer (PML) [1] is highly effective as an absorbing boundary condition (ABC) for the FDTD code. Several contributions highlighting its superior performance in many different applications have been published in the last two years. However, a careful choice of the shape of the conductivity to be used in the PML layers is necessary in order to obtain the best performance. In fact, while the PML material is theoretically reflection-less, in practice a numerical error depending on the grid cell-size for propagating waves should be taken into account. It is shown that the overall performance of the PML as ABC for the FDTD code depends on the reflection of the waves reflecting from the backing metal plane and on a numerical error depending upon the difference of the conductivity between two adjacent cells. An analytical expression to describe this error has been derived, and an inversion theory approach has been used to optimize the conductivity profile. Lastly, the effect of using PML in bioelectromagnetic simulations is discussed.

Optimization of the PML

The PML boundary condition has been implemented in the FDTD code with a conductivity profile given by

$$\sigma_i = \sigma_0 \frac{i^{n+1} - (i-1)^{n+1}}{n+1} \qquad (1)$$

with σ_0 a constant, i the cell number in the PML layer, and n the order of variation of the conductivity. The performance of the PML boundary has been tested following the same approach as described in [2]. Performance similar to that presented in [3] has been obtained, with the PML ABC capable of giving errors that are three to four orders of magnitude less than those obtained using the Mur 2nd order ABC [4]. Moreover, we have found that the performances of the Retarded Time [5] ABC are comparable to those of the Mur 2nd order. For our evaluation, we have considered an infinitesimal dipole placed in the center of a 50x50x50 cells mesh, at a frequency of 835 MHz, with cell size δ=2mm. The simulations have been run for 120 time steps, and we have considered the average of the local error along a line parallel to the boundary for several different cases [6]. The overall error along this line has been found to be given by the sum of the

0-7803-4178-3/97/$10.00 © 1997 IEEE

theoretical reflection of the PML backed by a metal plane and the third order error intrinsic in the approximation of the derivatives in the FDTD algorithm [6]. Therefore, the error can be expressed by

$$R = e^{-2Z_0\int_{0.5\delta}^{(m-0.5)\delta}\sigma(x)\,dx} + \frac{(\delta/2)^2}{6}\int_{0.5\delta}^{(m-0.5)\delta}\frac{\partial^3}{\partial x^3}e^{-Z_0\sigma(x)x}dx \qquad (2)$$

where Z_0 is the intrinsic impedance of vacuum, m the total number of PML layers used for the absorbing boundaries, and $\sigma(x)$ is the continuous form of (1), i.e.,

$$\sigma(x) = \sigma_0\frac{\left(\frac{x}{\delta}+1\right)^{n+1} - \left(\frac{x}{\delta}\right)^{n+1}}{n+1} \quad . \quad (3)$$

In (2), the error in the differential approximation has been integrated over the PML thickness to obtain the overall effect of the boundary. The limits in the integral have been chosen in order to take into account the stair-step approximation of the FDTD. It has been found that (2) is reasonably accurate in predicting the best order n to be used in (1). The average of the local error on the border line of the mesh plotted in Fig. 1a for the various boundaries and different values of the order n for the conductivity ($1.6 \le n \le 5.2$) can be compared to that in Fig.1b, obtained by using (2). Alternatively, it has been found to give accurate results the discrete formulation of (2), that is

$$R = e^{-2Z_0\delta\sum_{i=1}^{m}\sigma_i} + \frac{(\delta/2)^2}{6}\delta\sum_{i=1}^{m}Z_0^3\sigma_i^3 e^{-Z_0\sigma_i i\delta} \quad . \quad (4)$$

The interesting feature of (2) and (4) is that it is possible to search for alternative profiles of the conductivity by using an inverse theory approach. In particular, the Newton method can be used by appropriately altering the shape of the conductivity in an iterative algorithm. It is possible, therefore, to calculate from each iteration the Frechet derivative of the error given by (2) with respect of a vector variation of the profile of the conductivity in the PML. An alternate $\sigma(x)$ that minimizes the error given by (2) can then be found in a few iterations of the Newton method. This algorithm has been successfully applied, and performances better than, or comparable to, the best performance obtained by using a parabolic-like conductivity profile given by (1) have been obtained.

Application to Bioelectromagnetic Simulations

Although the PML ABC has been shown to be more accurate than Mur or RT ABCs, few results are available in the literature examining its use for realistic applications. In this paper, the optimized PML boundary condition has been applied to some bioelectromagnetic simulations in order to analyze the effect of having an extremely accurate ABC for these cases. One interesting application is the calculation of the radiation pattern and induced specific absorption rates (SARs) of mobile telephones in the

presence of the human head. For these simulations, we have found that the PML ABC gives results within 1% compared to those obtained by using Mur or RT ABCs. As an example, Fig.2 shows a comparison of the radiation pattern of a 835MHz cellular telephone in the presence of the human head comparing RT and PML as ABCs. As can be seen, the two results are quite similar.

The PML has been used also for low-frequency applications. Fig.3, for example, shows the electric field components in a 2/3 muscle equivalent sphere (σ=0.35 S/m) illuminated by a 20 MHz plane-wave (E_{inc}=1 V/m), scaled to 60 Hz. In this case, PML provides slightly better results that compare well with the analytical solution. The PML boundary required very similar computational time and memory to the RT ABC for these simulations, as only 1-cell air space was required between the object and the PML boundary, whereas 9 cells were used for the RT boundary

Conclusions

An optimization technique for the PML ABC has been presented. The analytical approach to predict the theoretical reflection introduced by a PML backed by a metal plane has been used to determine optimized profiles for the conductivity of the PML material. The optimized PML has been used for several bioelectromagnetic applications, and only small differences have been found to date between the results obtained by using this boundary and traditional boundary conditions like RT or Mur.

References

1. J. P. Berenger, "A Perfect Matched Layer for the Absorption of Electromagnetic Waves," *J. Computational Physics*, 114, pp. 185 - 200, 1994.
2. T. G. Moore, J. G. Blashak, A. Taflove, and G. A. Kriegsmann, "Theory and Applications of Radiation Boundary Operators," *IEEE Trans. on Antennas and Propagation*, Vol. 36, pp. 1797 - 1812, 1988.
3. D. S. Katz, E. T. Thiele, and A. Taflove, "Validation and Extension to Three Dimensions of the Berenger PML Absorbing Boundary Condition for FD-TD Meshes," *IEEE Microwave and Guided Wave Letters*, Vol. 4, pp. 268 - 270, 1994.
4. G. Mur, "Absorbing Boundary Conditions for the Finite-Difference Approximation of the Time-Domain Electromagnetic-Field Equations," *IEEE Transactions on Electromagnetic Compatibility*, Vol. 23, pp. 377 - 382, 1981.
5. S. Berntsen, and S. N. Hornsleth, "Retarded Time Absorbing Boundary Conditions," *IEEE Transactions on Antennas and Propagation*, Vol. 42, pp. 1059-1064, 1994.
6. G. Lazzi and O. P. Gandhi, "On the Optimal Design of the PML Absorbing Boundary Condition for the FDTD Code," *IEEE Transactions on Antennas and Propagation*, Apr.1997.

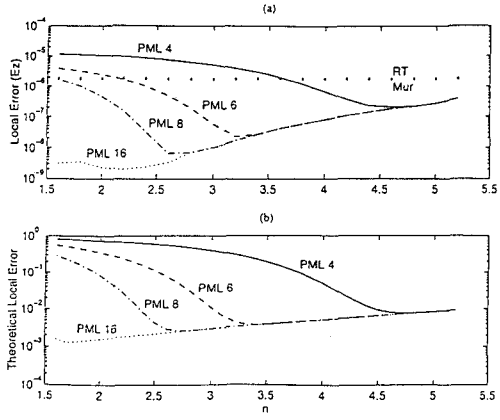

Fig.1. (a) Average of the local error along a line parallel to the boundaries as a function of the order n; (b) the numerically computed curves for the estimation of the best order n for the various PML boundaries

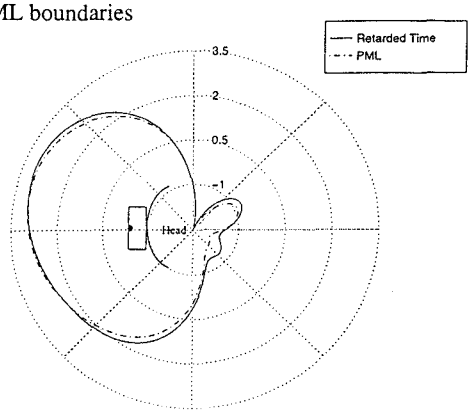

Fig.2. Comparison of the radiation patterns of an 835MHz cellular telephone obtained by using RT and PML boundary conditions

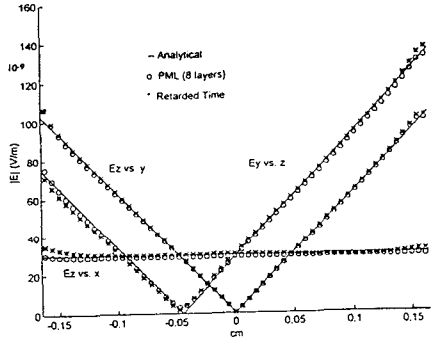

Fig.3. Comparison of the electric fields induced in a 2/3 muscle equivalent sphere illuminated by a 60Hz (scaled from 20MHz) plane wave of E_{inc}=1 V/m for RT and PML boundaries.